Photochemistry and Photobiology, 2009, 85: 261–271

Sensitivity of Erythemally Effective UV Irradiance and Daily Exposure to Temporal Variability in Total Ozone

Alois W. Schmalwieser*[1], Thilo Erbertseder[2], Günther Schauberger[1] and Philipp Weihs[3]

[1]Institute of Medical Physics and Biostatistics, University of Veterinary Medicine, Vienna, Austria
[2]Deutsches Fernerkundungsdatenzentrum, Deutsches Zentrum für Luft- und Raumfahrt, Oberpfaffenhofen, Germany
[3]Institute of Meteorology, University of Natural Resources and Applied Life Sciences, Vienna, Austria

Received 18 January 2008, accepted 9 June 2008, DOI: 10.1111/j.1751-1097.2008.00431.x

ABSTRACT

The provision of information to the public about current levels of the erythemally effective UV radiation is an important issue in health care. The quality of promoted values is therefore of special importance. The atmospheric parameter which affects the erythemally effective UV radiation under clear sky most is the total ozone content of the atmosphere. In this paper we examined the sensitivity of the erythemally effective irradiance and daily radiant exposure to the temporal variability of total ozone on time scales from 1 to 15 days. The results show that the sensitivity is highest for the first 24 h. Larger time scales do not exhibit a similar influence. Total ozone measurements of the previous day may already cause uncertainties higher than 0.5 UV index (UVI) independent of the geolocation. For comparison, a temporal persistence of 15 days may cause uncertainties of 1.2 UVI at 50°N, 1 UVI at 30°S and less than 1 UVI at the equator. The results of this study allow finding the necessary temporal resolution of total ozone values when a certain accuracy for the UVI or for the purpose of sun protection is required. The results are compared with those of two preceding studies where we quantified the influence of measurement uncertainties and spatial total ozone variability to the erythemally effective irradiance at noon and to the daily dose. We conclude that temporal variability of total ozone is the most critical issue, but also measurement uncertainties do have a noticeable influence on the erythemally effective radiation.

INTRODUCTION

Sun care nowadays is an important issue in health care. Information for the public about the current intensity of UV radiation may therefore be very helpful. The quality of published values is a critical issue and it is essential to know the accuracy of the promoted values. As evident from several studies (*e.g.* 1,2) the total ozone column (TOC) of the atmosphere is the most critical input parameter for calculations of the UV radiation under clear sky (cloud and aerosol free) conditions. In turn, uncertainties in TOC influence the accuracy of calculated values.

Uncertainties in TOC values result from limited accuracy of the intrinsic measurements, from limited spatial coverage and limited temporal availability, *i.e.* resolution. The magnitude of these uncertainties depends on a variety of parameters like measuring technique, ozone retrieval scheme, atmospheric dynamics, solar zenith angle and others.

In a previous paper we studied the effects of the intrinsic uncertainties of TOC measurements to calculated values of the erythemally effective irradiance at noon and daily radiant exposure (3). In a follow-up paper we examined the effects of uncertainties due to limited spatial resolution of TOC measurements (4). In this paper we investigate the influence of the temporal total ozone variability on time scales from 1 to 15 days on the erythemally effective UV irradiance at solar noon and daily exposure under clear sky conditions. We aim at quantifying the influence of total ozone data with a limited temporal resolution or temporal lags and the effect of assuming persistency of total ozone.

The temporal variability of TOC is caused by a variety of phenomena on a broad spectrum of temporal and spatial scales. Generally, ozone distribution is determined by photochemical production, transport and destruction. A strong annual or semiannual cycle builds the most obvious pattern in the temporal course of TOC on both hemispheres. The annual cycle reaches its maximum in the winter and spring months and its minimum in the autumn months. The amplitude depends strongly on latitude. In the tropics the semi annual cycle is most obvious and corresponds clearly to solar elevation.

For periods up to 15 days, however, phenomena that affect TOC at subsynoptic and synoptic scales are most important. These subsynoptic and synoptic fluctuations, the classical weather–ozone relations, amount up to 10% of the total column in the tropics and up to 30% in middle and high latitudes. These fluctuations are known since the pioneering work of Dobson (5,6), Meetham (7) and Reed (8). Depending on geolocation, these fluctuations can change the TOC amount by more than 100 DU within 24 h and hence govern the short-term variability of TOC. Short-time fluctuations of TOC for a time span of 2 days around the globe were estimated by Schmalwieser *et al.* (9) using correlation analysis. It was shown that low correlation coefficients are found at mid and high latitudes, and that the coefficients increase toward higher and lower latitudes.

*Corresponding author email: alois.schmalwieser@vu-wien.ac.at (Alois W. Schmalwieser)

To a much lower extent, but for the sake of completeness, contributions to the temporal variability of TOC within 15 days result from the quasi-biennial oscillation (QBO), regional El Niño/La Niña effects, volcanic eruptions and the solar activity cycles.

Changes in solar activity affect the ozone forming UV irradiance. The 11-year solar cycle (*e.g.* 10–12) may cause variations in TOC of the order of 4% relative to a long-term mean. The TOC reaches maximum values near sunspot maxima and can be identified best at the tropics. The 27-day solar rotation is seen as similar change (*e.g.* 11,13) of the order of a few percent. The amplitude of the QBO signal in TOC (14) depends on latitude and season and can reach up to 8% of the annual mean (*e.g.* 13,15,16).

Effects from the El Niño/La Niña Southern Oscillation occur on a time scale from 3 to 7 years (*e.g.* 17), and exhibit a duration from 7 to 8 months. Its effect on TOC variability shows zonal asymmetry and may cause a reduction in TOC of the order of −4%. Large volcanic eruptions can lead to significant radiative/chemical and dynamical changes which may lead to declines as large as −5% (*e.g.* 18) over a period of a few years. Finally, the North Atlantic Oscillation and the Arctic Oscillation (*e.g.* 19) induce clear signatures on synoptic scale fluctuations of TOC over the Euro-Atlantic sector (20,21) and higher latitudes, respectively, and may be responsible for the enhanced appearance of ozone miniholes (22).

In this paper we investigate the sensitivity of the erythemally effective irradiance and daily radiant exposure to short-term fluctuations of TOC on time scales up to 15 days depending on the season. The sensitivity to temporal variability can also be interpreted as the constraint of accuracy due to a limited temporal resolution, availability or the uncertainty which may arise from assuming persistency. The study is carried out aiming at sun care and public health. For this, the values of the erythemally effective irradiance are expressed in units of the UV Index (UVI) as proposed by several organizations (23–27). In case of the daily dose, UVI hours (UVIH) are used as unit following a suggestion of Saxebøl (28). Regarding radiation protection and health care we use the 95th percentile (p95) as the measure of relevance for the analysis.

Additionally, this study allows to estimate the necessary properties of TOC if a certain accuracy of the UVI or of a recommendation for sun protection, like the sun protection factor, is required.

MATERIALS AND METHODS

The uncertainties in the erythemally effective UV radiation from a restricted temporal resolution are estimated by analyzing the differences resulting from temporally shifted TOC time series as input parameter. Differences due to lags in TOC between 1 day and 15 days were calculated and analyzed.

TOC data. In order to be consistent with two related preceding papers (3,4), the TOC data have been taken from the Total Ozone Mapping Spectrometer (TOMS) on board NASA's Earth Probe satellite (EPTOMS) for this study, too. TOMS measures incident solar radiation and backscattered ultraviolet sunlight at six near-UV wavelengths and TOC values are retrieved from these measurements (29,30). The measurements are taken close to solar noon. We use the gridded level-3 near-real time data. These data are given on a 1° latitude by 1.25° longitude grid containing 180×288 grid points at global coverage. We apply gathered near-real time data, which were processed by TOMS Version 7.

The analysis is based on time series of EPTOMS total ozone observations at the following geolocations: 50.0°N and 15.6°E (Solar and Ozone Observatory at Hradec Kralove, Czech Republic); 0.0°N and 36.6°E (ozone observatory near Nairobi, Kenya); and 30.0°S and 18.1°E (ozone observatory near Springbok, South Africa). To be consistent with the related earlier work we have included all available observations between 1 January 2000 and 31 December 2004. The ongoing problems in calibration of EPTOMS in 2004 did not affect our analysis. This was proved by analyzing the statistical parameters for each single year (see below).

Uncertainty analysis. In order to quantify the influence of temporal variability in TOC data on the erythemally effective radiation, we performed model calculations with a fast spectral UV radiation model. This model was developed by some of us (31) improving the suggestion of Diffey (32). It uses the data base from Bener (33) which was obtained from spectral measurements made over several years at Davos (46°48′N, 9°49′E, 1590 m a.s.l.) for parameterization. The model setup is similar to that used in the two related previous papers. A more detailed description of the model can be found in Schmalwieser *et al.* (34).

The erythemally effective irradiance is gained by using the CIE (Commission Internationale de l'Eclairage) action spectrum of the erythema (35) for weighting followed by the integration over the whole spectral range and expressed in units of the UVI where 1 UVI corresponds to 0.025 $W_{eff}\ m^{-2}$. The daily radiant exposure (or daily dose) is gained by integrating the daily course of the effective irradiance from sunrise to sunset and is expressed in units of UVIh following a suggestion of Saxebøl (28) where 1 UVIh corresponds to 90 $J\ m^{-2}$ (0.9 SED) (36).

The model was validated with respect to the erythemally effective UV radiation by comparison with other models (37–39) and comparison with measurements made at four different continents for irradiance (35) and daily dose (40).

To be consistent with our two related previous papers an aerosol pure atmosphere and a cloud-free sky was assumed to point out the maximum influence as this is important for radiation protection. Therefore, the input parameters comprise date, time, geographical position, altitude and TOC.

The uncertainties in the erythemally effective radiation resulting from limitations in accuracy due to temporal lags were estimated by consecutively inputting temporally shifted time series of TOC to the model. First, the erythemally effective irradiance was calculated for a certain location and a certain day with the temporally correct TOC value. It was then calculated by using time series of TOC shifted between 1 and 15 days. For each day of the 5 year period such a time series was calculated. Finally, the absolute differences between the current value and the shifted time series were calculated for each day of the 5 year period.

Differences in TOC are derived similarly. Differences are calculated between the current value and the shifted time series. Additionally the differences were set in relation to the current value and expressed in percentage.

The statistical analysis of the obtained differences was carried out by using the p95 of absolute differences for each month of the year as the main indicator. The p95 value indicates the difference or uncertainty that is exceeded at one day of the month. The statistical analysis is completed using the 50th percentile (p50) and the 100th percentile (p100). The p50 value denotes the median, *i.e.* the difference that is exceeded on 50% of the days. The p100 values quantifies the highest difference found over the 5 year period for a given month. The analysis is performed separately for daily maximum irradiance (solar noon), daily dose under clear sky conditions and TOC.

RESULTS

Influence of temporal total ozone variability at 50°N

At 50°N (Hradec Kralove, Czech Republic) the TOC exhibits high temporal variability throughout the year with values from 200 to 500 DU. Significant changes by more than 100 DU within 24 h can be observed. Solar height at noon varies between 17° in winter and 63° in summer. With these, the erythemally effective irradiance at solar noon under clear sky varies from 0.5 UVI (winter) to 7 UVI (summer). The length of the day undergoes large changes of more than 8 h. The daily dose under clear sky may be below 2 UVIh in winter and can exceed 50 UVIh near the summer solstice. Visualizations of TOC values, erythemally effective irradiance at noon and daily dose can be found in Schmalwieser *et al.* ([3] 1997–1999) and Schmalwieser *et al.* ([4] 2000–2004).

The temporal variability analysis of TOC at the p50 and p95 level (Figs. 1a and 2a) shows a clear annual cycle with higher values during late winter/early spring and lower values during

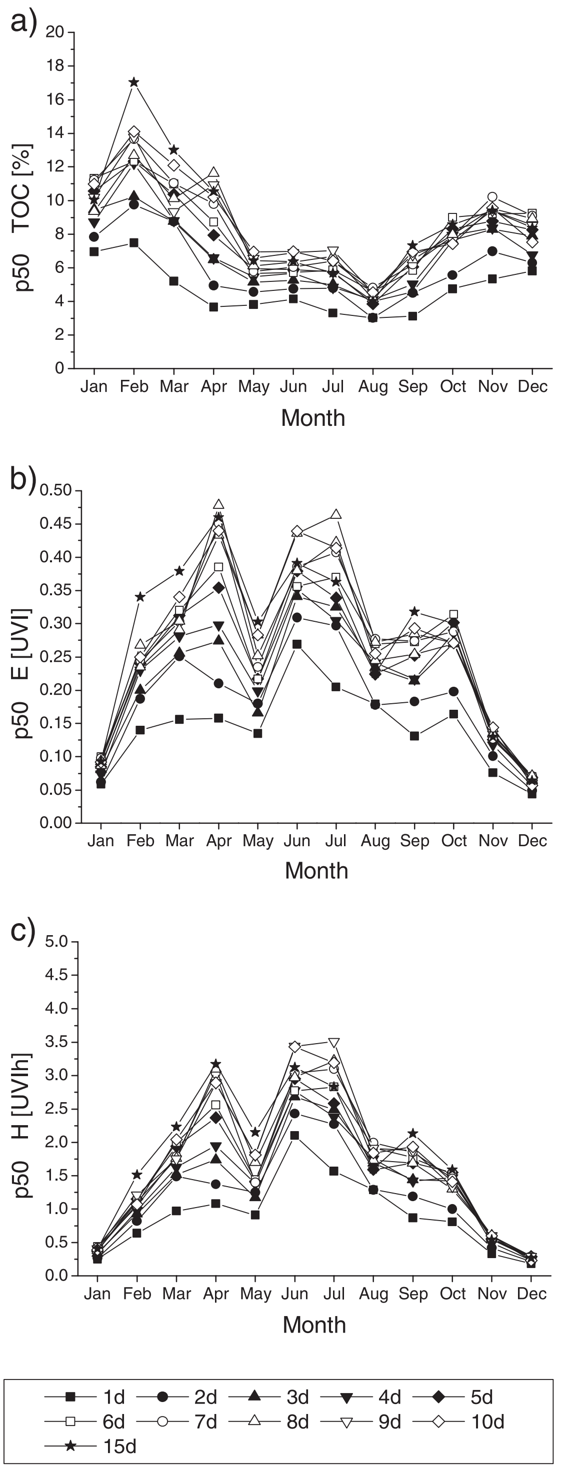

Figure 1. Fiftieth percentiles for absolute differences in total ozone p50ΔTOC (a), irradiance at solar noon p50Δ*E* (b) and daily dose p50Δ*H* (c) at 50.0°N, 15.6°E (near Hradec Kralove, Czech Republic) under clear skies for certain temporal lags up to 15 days.

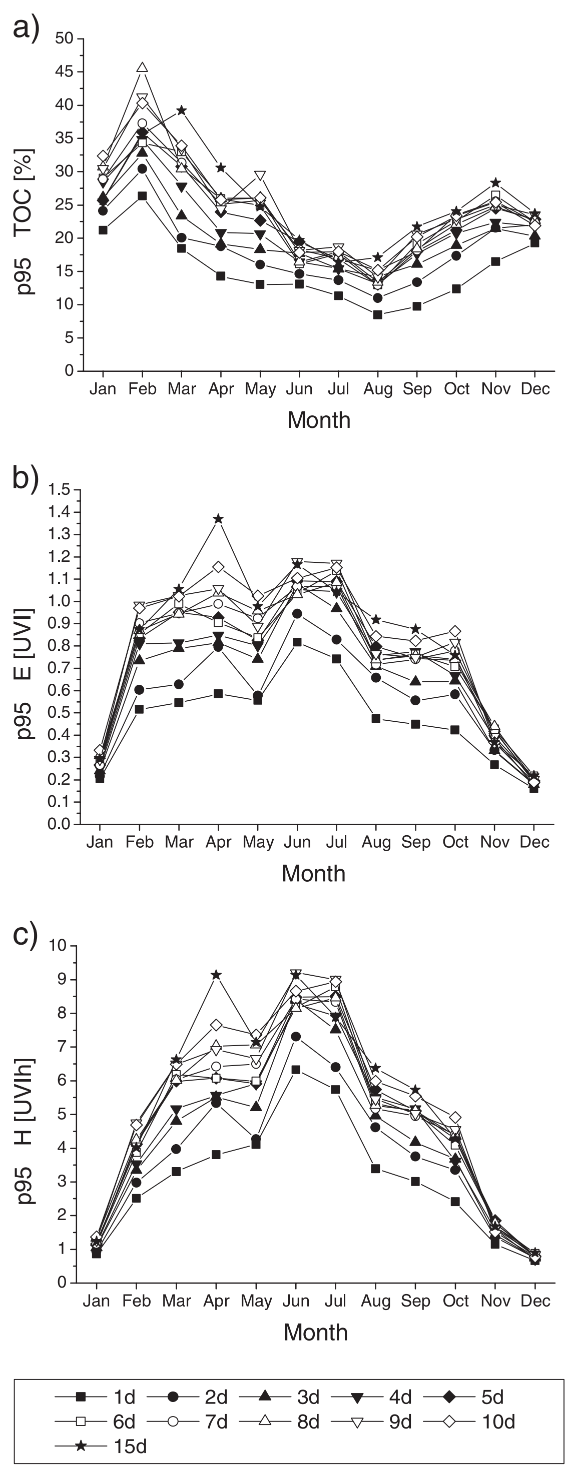

Figure 2. Ninety-fifth percentiles for absolute differences in total ozone p95ΔTOC (a), irradiance at solar noon p95Δ*E* (b) and daily dose p95Δ*H* (c) at 50.0°N, 15.6°E (near Hradec Kralove, Czech Republic) under clear skies for certain temporal lags up to 15 days.

summer. Only for the shorter time lags there is a clear relationship between the p50 or p95 value and the lag. The longest lags do not necessarily cause the highest uncertainty values. The increase in the differences is rather low as the values for a lag of 15 days are approximately twice as high as for a lag of 1 day only. The highest monthly differences in TOC (p100) due to time lags found within the 5 year period (Fig. 3a) show a clear annual course but only a weak relationship between their magnitude and the underlying time lag. Similar to the above, they are highest in spring and lowest in summer. From one day to another TOC may vary by 15% in summer and 40% in spring. Within a week changes up to 70% can be observed in spring which corresponds to more than 100 DU.

The p50 values of the erythemally effective irradiance at noon exhibit a dual pattern (Fig. 1b). During spring the pattern is dominated by the higher temporal variability of TOC due to high dynamic activity in the atmosphere. An influence from solar height cannot be seen. From May to August the pattern is dominated by the annual course of solar height. Late summer and fall are then again strongly influenced by the increasing dynamic activity and the influence of solar height becomes invisible again. The changes from variability as main influence to solar height and vice versa become obvious by the relatively low values in for May and August. Further, the pattern changes with progressing time lag. For longer temporal delays the increase is much lower than within the first day. The annual behavior of p95 (Fig. 2b) and p100 (Fig. 3b) is similar but the influence of high variability in late winter and spring (February–May) becomes stronger. The p100 values are almost constant from February to August at a level of 1 UVI for a lag of 24 h. In the p95 the corresponding values are above 0.5 UVI from February to July.

In the absolute differences for the daily dose (Figs. 1c, 2c and 3c) the duality is still evident but the length of the day dominates the pattern significantly.

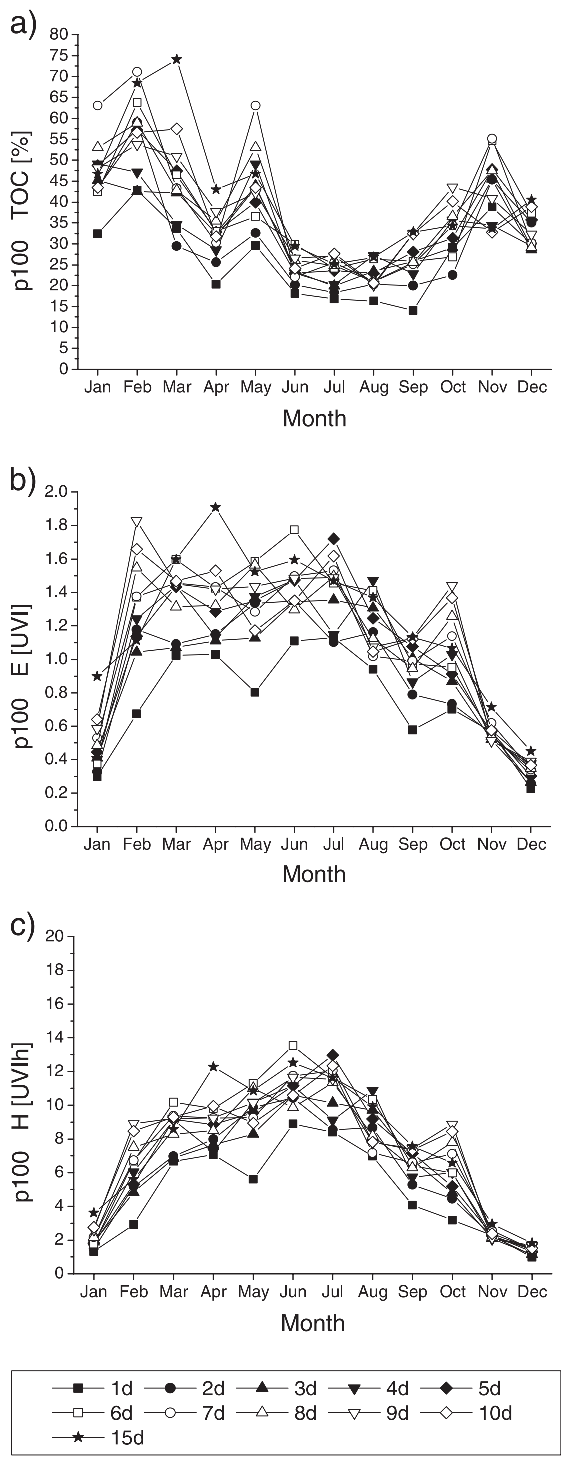

Figure 3. Hundredth percentiles for absolute differences in total ozone p100ΔTOC (a), irradiance at solar noon p100ΔE (b) and daily dose p100ΔH (c) at 50.0°N, 15.6°E (near Hradec Kralove, Czech Republic) under clear skies for certain temporal lags up to 15 days.

Influence of temporal total ozone variability at 30°S

At 30°S (near Springbok, South Africa) the TOC varies by 150 DU during the year where a clear annual cycle can be observed. The lowest values are around 225 DU and are measured near the winter solstice (June). The highest are observed in spring and are of the order of 375 DU. Day-to-day variability is up to 70 DU.

The erythemally effective irradiance at solar noon under clear skies is within 2 UVI (winter) and 10 UVI (summer). The daily dose undergoes annual changes from 10 to 65 UVIh. Visualizations of TOC values, erythemally effective irradiance and daily dose can be found in Schmalwieser *et al.* ([3] 1997–1999) and Schmalwieser *et al.* ([4] 2000–2004).

The p50 values of the absolute differences (Fig. 4a) caused by temporal variability of TOC reveal an annual course with highest values around August and lowest values around January and February. An increase in the p50 and p95 values with increasing lag can be detected up to lags of 3 or 4 days. In some cases there is a further increase with longer lags but there are also some months where longer lags cause lower differences. The relationship between the p100 value and the length of the lag is weaker than for the p50 and the p95 values. The highest values at certain months are induced even by a temporal lag of 6 (p50), 4 (p95) or 7 (p100) days.

The temporal variability in TOC influences the annual course of p50 for the erythemally effective irradiance (Fig. 4b). The highest values can be found in the months before the summer solstice (December), between August and November. A temporal lag of 1 day in TOC produces an uncertainty at the p50 level between 0.12 UVI (May) and 0.25 UVI (November). The highest p50 values are 0.37 UVI in August from a lag of 6 days and 0.38 UVI in November from a lag of 15 days.

The length of the day weakens the influence of the temporal variability of TOC less and the highest values can still be found before the summer solstice (Fig. 4c). A temporal lag in TOC of 1 day results in a p50 of 0.75 UVIh in June and July and a value of 1.75 UVIh in November. The highest p50 value of all is found in November for a lag of 15 days. During most months, however, the highest p50 value is caused by shorter lags.

The p95 in the erythemally effective irradiance at noon (Fig. 5b) within the first 24 h goes up to 0.4 UVI in April and

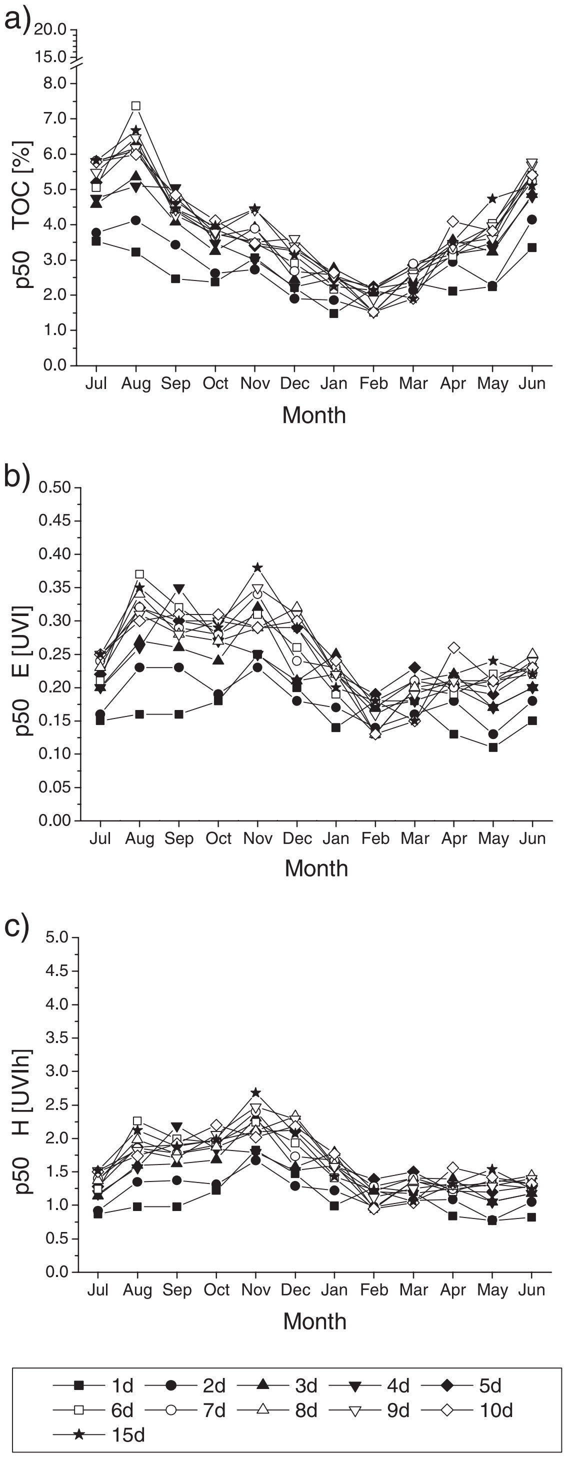

Figure 4. Fiftieth percentiles for absolute differences in total ozone p50ΔTOC (a), irradiance at solar noon p50ΔE (b) and daily dose p50ΔH (c) at 30.0°S, 18.1°E (near Springbok, South Africa) under clear skies for certain temporal lags up to 15 days.

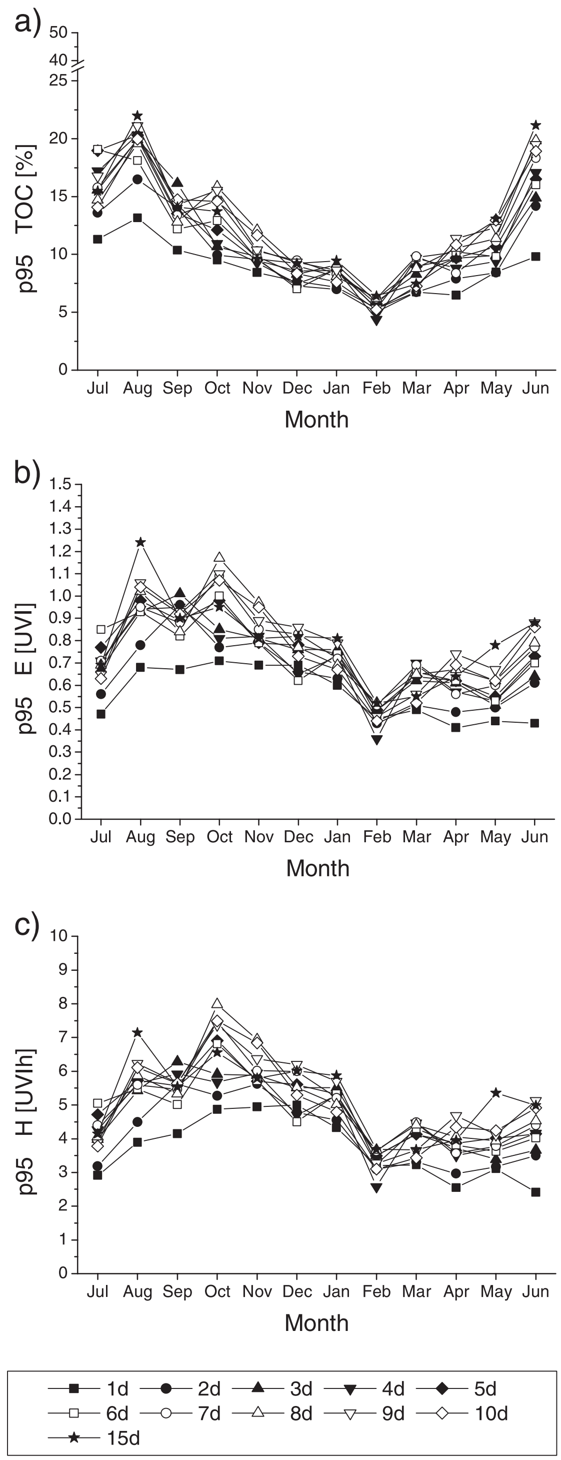

Figure 5. Ninety-fifth percentiles for absolute differences in total ozone p95ΔTOC (a), irradiance at solar noon p95ΔE (b) and daily dose p95ΔH (c) at 30.0°S, 18.1°E (near Springbok, South Africa) under clear skies for certain temporal lags up to 15 days.

0.7 UVI in October. For the daily radiant exposure (Fig. 5c) the values are within 2.5 UVIh (June) and 5 UVIh (December). Except for September, the highest p95 values are caused by lags longer than 8 days. The annual pattern of the p95 in irradiance as well as in daily dose peaks obviously before the summer solstice and is therefore much more influenced by the temporal variability of TOC than the p50 values are.

For the erythemally effective irradiance at noon the p100 values (Fig. 6b) do not show a clear annual course and only the shortest lag gives the lowest p100 values. They are between 0.6 and 1.2 UVI with no tendency for a certain season. The highest p100 around 1.8 UVI are seen in October and November and are caused by lags in TOC of 10 or 15 days. However, lags of 3 or 4 days may cause p100 values around 1.6 UVI.

A lag of 1 day causes p100 values between 4.5 UVIh (April) and 8 UVIh (November) as can be seen from Fig. 6c. As in the case of irradiance, temporal lags of 3 days may cause as high p100 values than lags of 10 or 15 days.

Influence of temporal total ozone variability at the equator

At the equator (Nairobi, Kenya) the TOC changes by less than 100 DU during the year, *i.e.* between 220 and 300 DU. This amplitude is of the order of changes that can occur within a day at 50°N. Day-to-day variations in TOC can be as high as 40 DU. Further, the change in solar zenith angle at noon is within ±23°. Therefore, irradiance at solar noon varies by only 3 UVI units during the year having one maximum in March and one in September around 10.5 UVI. Accordingly, the daily dose undergoes smooth changes within 45 and 65 UVIh. Visualizations of TOC values, erythemally effective irradiance and daily dose can be found in Schmalwieser *et al.* ([3] 1997–1999) and Schmalwieser *et al.* ([4] 2000–2004).

For the differences in TOC at Nairobi (Fig. 7a) no relationship between the length of the temporal lag and the p50 value can be found. The annual course of p50 does not exhibit an obvious pattern. Values are between 1.0% and 3.25% with a slight tendency to be highest in November.

For the erythemally effective irradiance at noon the p50 values (Fig. 7b) caused by temporal lags in TOC the annual course is very similar to that of TOC as solar height at noon does not change much during the year. Values range from 0.10 UVI to just above 0.25 UVI. The same characteristic is exhibited by the p50 in daily exposure (Fig. 7c). The p50 values are within 0.6 and 1.9 UVIh.

A relationship between the temporal distance and the p95 value is slightly distinguishable for the absolute differences in TOC (Fig. 8a). The lowest values of 3.5% are found for a lag of 2 days in June and September. The highest values of 9.5% are caused by a temporal lag of 7 days in November.

The p95 values for irradiance (Fig. 8b) and daily dose (Fig. 8c) show a smooth annual course. Similar to that at the other locations, the increase in p95 is highest within the first 24 h, but on the contrary there is almost no further increase in the p95 values with increasing temporal lag. For a lag of 1 day the p95 oscillates around a value of 0.55 UVI or 3.5 UVIh. For lags of 10 days the p95 values are of the order of 0.65 UVI or 4 UVIh.

For the differences in TOC at the p100 level (Fig. 9a) a relationship to the temporal distance is slightly noticeable but not for each month of the year.

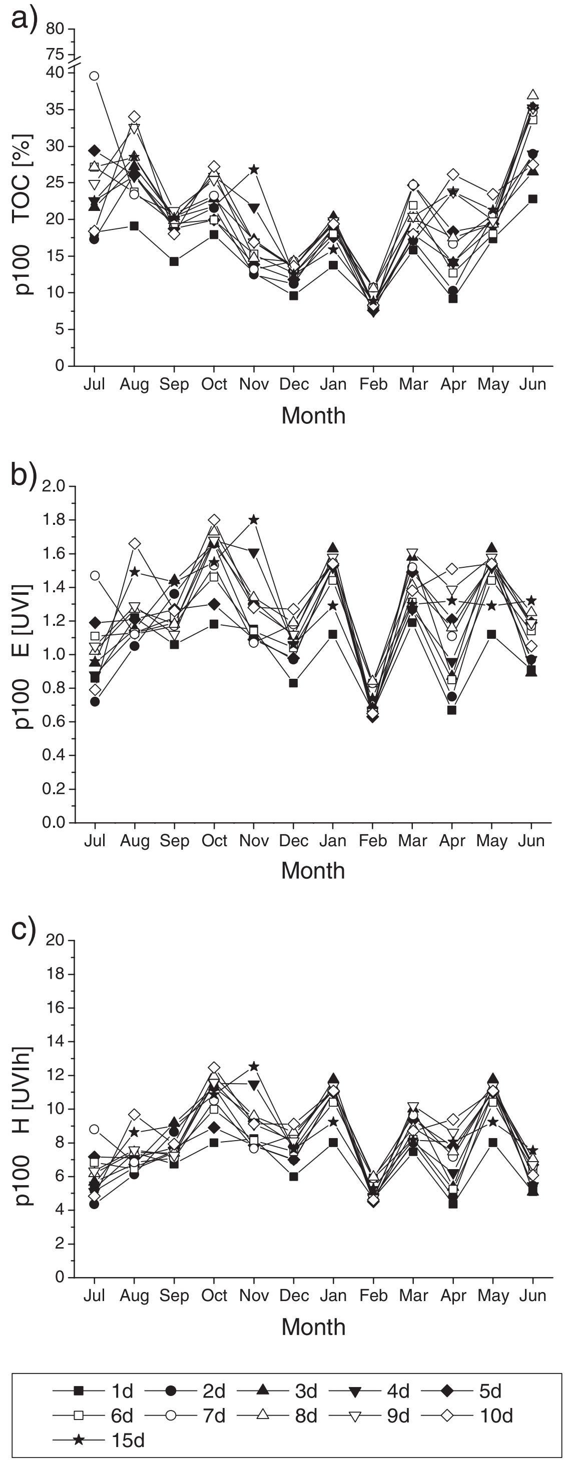

Figure 6. Hundredth percentiles for absolute differences in total ozone p100ΔTOC (a), irradiance at solar noon p100ΔE (b) and daily dose p100ΔH (c) at 30.0°S, 18.1°E (near Springbok, South Africa) under clear skies for certain temporal lags up to 15 days.

For irradiance at noon the p100 (Fig. 9b) is between 0.5 and 1.5 UVI, hence a lag of 1 day may result in a value above 1 UVI (January).

The p100 values for daily dose (Fig. 9c) are all above 2.5 UVIh and a lag of 1 day may result in a value of 9 UVIh (January). For the others the p100 values may go up to 11 UVIh.

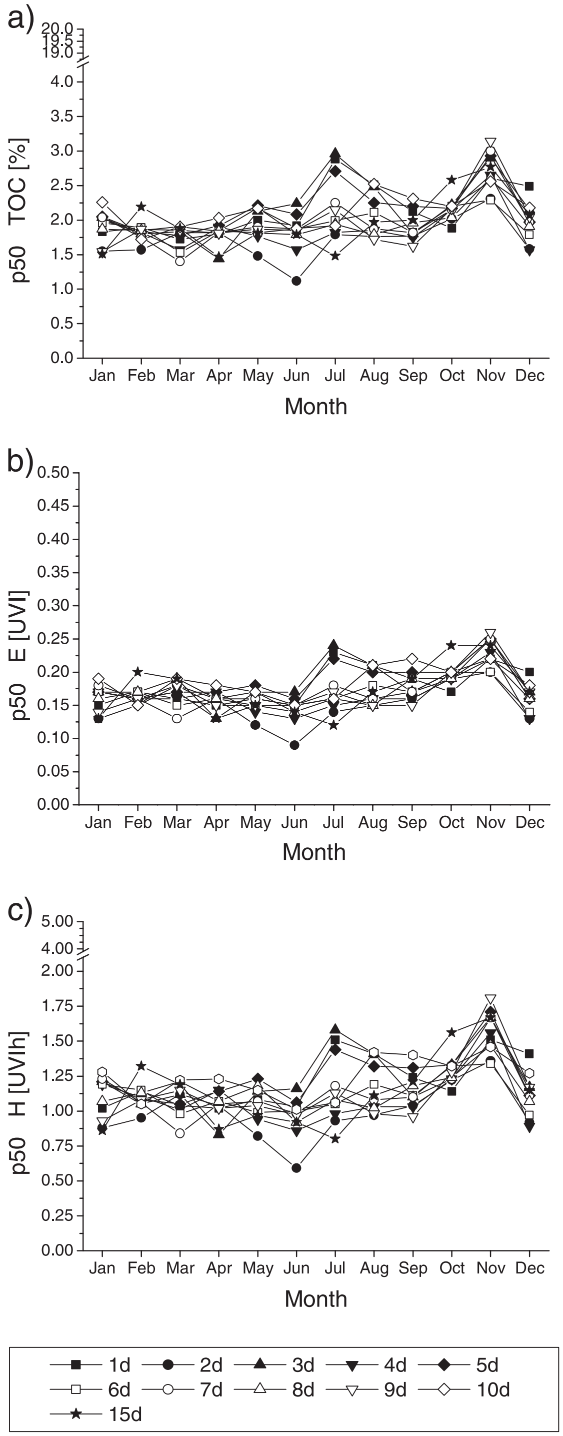

Figure 7. Fiftieth percentiles for absolute differences in total ozone p50ΔTOC (a), irradiance at solar noon p50ΔE (b) and daily dose p50ΔH (c) at 0.0°S, 36.6°E (near Nairobi, Kenya) under clear skies for certain temporal lags up to 15 days.

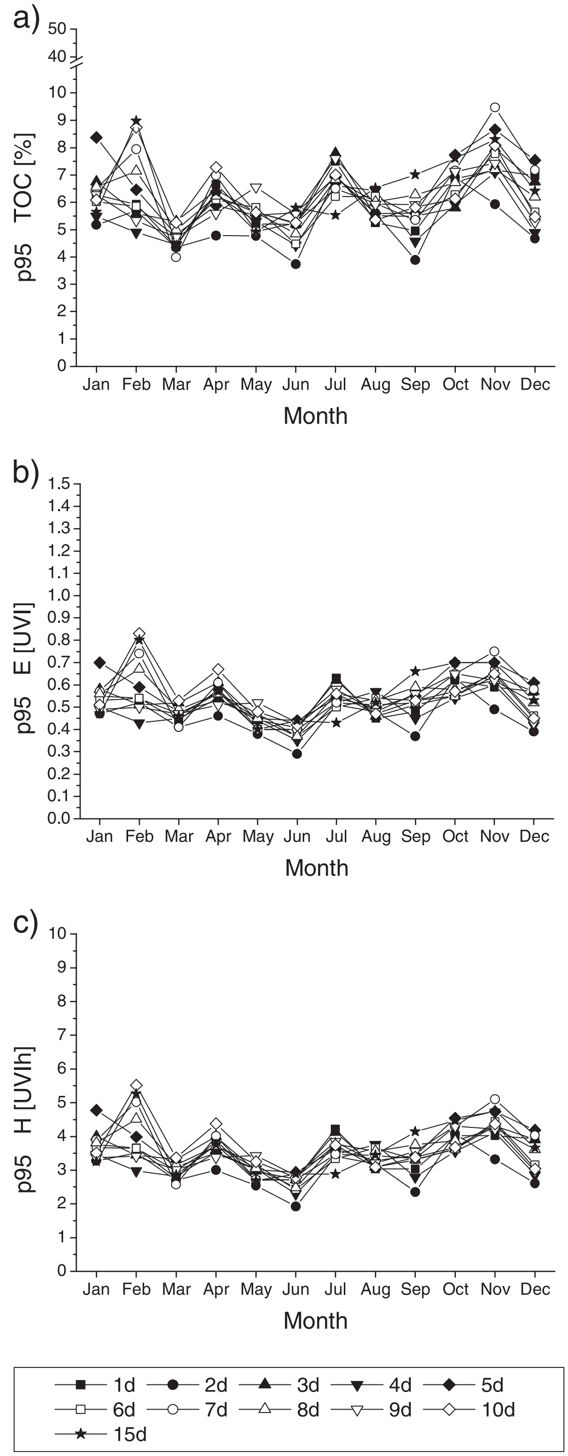

Figure 8. Ninety-fifth percentiles for absolute differences in total ozone p95ΔTOC (a), irradiance at solar noon p95ΔE (b) and daily dose p95ΔH (c) at 0.0°S, 36.6°E (near Nairobi, Kenya) under clear skies for certain temporal lags up to 15 days.

DISCUSSION

The accuracy of calculations of the erythemally effective UV radiation (E) is strongly limited by the temporal and spatial availability and resolution as well as the accuracy of measured TOC values. In this paper we have studied the influence of temporal variability of TOC on the erythemally effective UV radiation. We have quantified the uncertainties which are introduced when using TOC values with a certain temporal delay, the influence of time lags and the effect of assuming temporal persistency of TOC for periods up to 15 days.

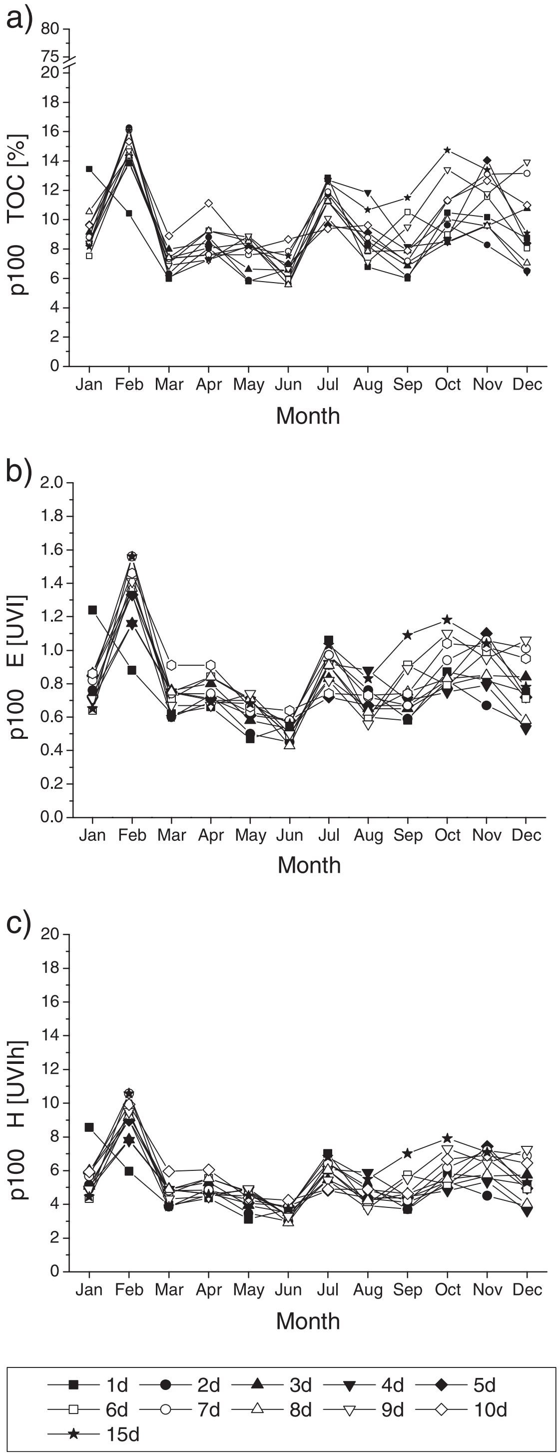

Figure 9. Hundredth percentiles for absolute differences in total ozone p100ΔTOC (a), irradiance at solar noon p100ΔE (b) and daily dose p100ΔH (c) at 0.0°S, 36.6°E (near Nairobi, Kenya) under clear skies for certain temporal lags up to 15 days.

As in two related preceding papers, where we estimated the influence of measurement uncertainties and uncertainties due to spatial variability of TOC, we performed this analysis with special emphasis on the UVI and sun protection. When promoting the UVI as integer one can use values of 0.5 and 1 UVI as thresholds for inaccuracy. Accordingly, an equivalent to the minimal erythema dose (MED) for melano-compromised (fair-skinned) persons (Fitzpatrick skin Type I and II) (24,41) and its manifolds can be used as threshold for radiant exposure (daily dose) (H). Expressed in units of UVIh, 1 MED is close to 2.5 UVIh and denotes a difference in the sun protection factor of 1.

The study enables to estimate the maximum length of lags/gaps in TOC time series in order to stay below a certain threshold of accuracy for a quantity related to sun protection. For this, we have chosen the p95 of the absolute differences as an indicator of uncertainty as it indicates the error that is reached on 1 day in a month.

At first glance one could expect increasing differences with increasing time lags in TOC or persistency of TOC. Thus, the most surprising outcome of our analysis is that the influence of time lags does not increase much with lag length. At each geolocation and for all percentiles the uncertainty due to temporal variability is relatively highest within the first 24 h. For longer lags the further increase is much lower and even vanishing. The explanation is quite simple; the classical ozone–weather relationship resulting in large day-to-day variations in TOC is the dominating factor for periods up to 15 days.

At 50°N an uncertainty of 0.5 UVI for E and 2.5 UVIh for H is exceeded at least during 6 months a year at the p95 level. For E a lag of 5 days can cause a difference of 1 UVI in June and July; but for time lags of 15 days the maximum remains below 1.2 UVI at the p95 level. For H the uncertainties stay below 10 UVIh. However, a lag of 1 day may result already in 5 UVIh.

At 30°S an uncertainty of at least 0.5 UVI for E and 2.5 UVIh for H has to be taken into account throughout the year by a lag of 1 day only. For E an uncertainty >1 UVI only occurs in August and October caused by lags longer than 7 days. For H the highest p95 values reach 7.5 UVIh for an 8-day lag.

At the equator temporal lags in TOC may result in uncertainties for E between 0.3 and 0.8 UVI. A clear relationship with respect to the length of the lag or a seasonal dependence cannot be inferred. The corresponding values for H vary from 2.5 to 5 UVIh.

To sum up, the temporal variability of TOC is highest at 50° and decreases with latitude. A lag or gap of 1 day in TOC measurements may cause an uncertainty of more than 0.5 UVI for E and 2.5 UVIh for H at all locations. Therefore, an uncertainty of 1 UVI for E and 5 UVIh for H should be taken into account. For temporal lags up to 15 days uncertainties stay below 1.5 UVI and 10 UVIh.

If we compare these results with the findings of a previous study on the influence of total ozone measurement uncertainties to the erythemally effective radiation (13), we can infer that at 50°N the impact of a time lag of 1 day is higher than the influence of measurement uncertainties (Fig. 10). The same can be concluded for 30°S (Fig. 11). At the equator, however, the influence of measurement uncertainties can be slightly lower or higher (Fig. 12) than that of a 1-day lag or gap.

In any case, a certain contribution of the observed variability within the first 24 h comes from measurement uncertainties. However, there is a noticeable difference between the annual courses of the p95 values from measurement uncertainties and from time lags. At 50° the difference is most

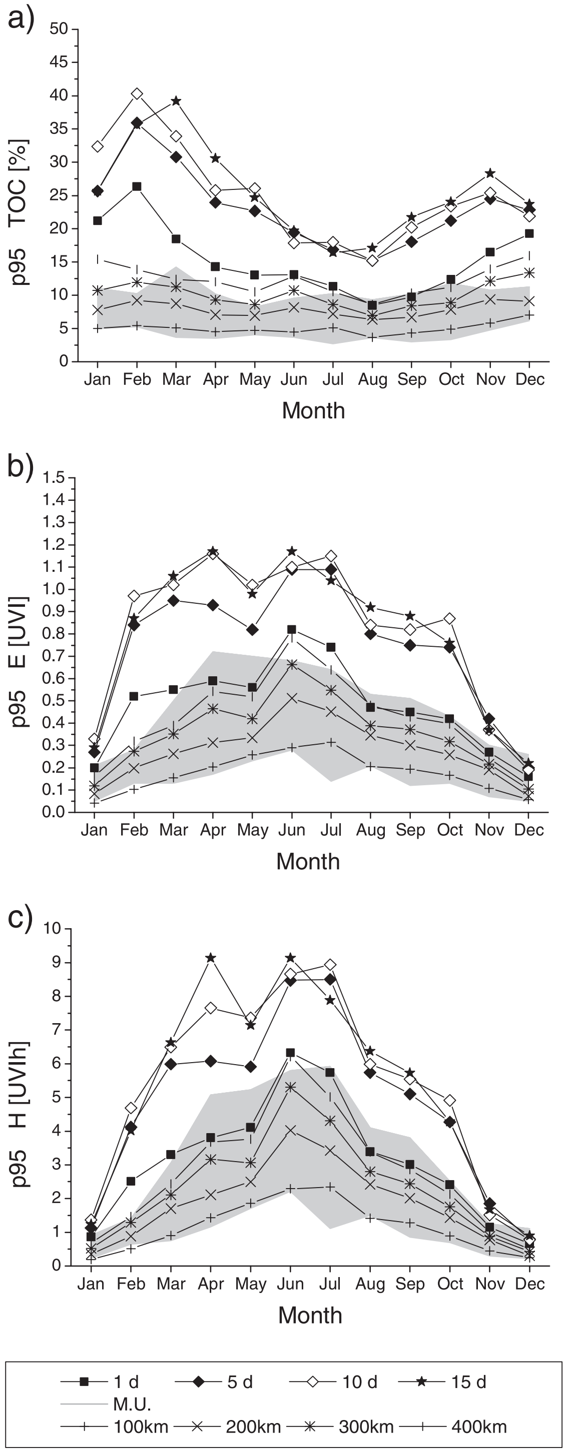

Figure 10. Ninety-fifth percentiles for absolute differences in total ozone p95ΔTOC (a), for irradiance at solar noon p95ΔE (b) and for daily dose p95ΔH (c) at 50.0°N, 15.6°E for certain temporal lags up to 15 days. The gray area indicates the measuring uncertainties of TOC and their influence on the erythemally effective UV radiation after Schmalwieser *et al.* (3). Shown are also the p95 values caused by the spatial (latitudinal) variability in TOC after Schmalwieser *et al.* (4).

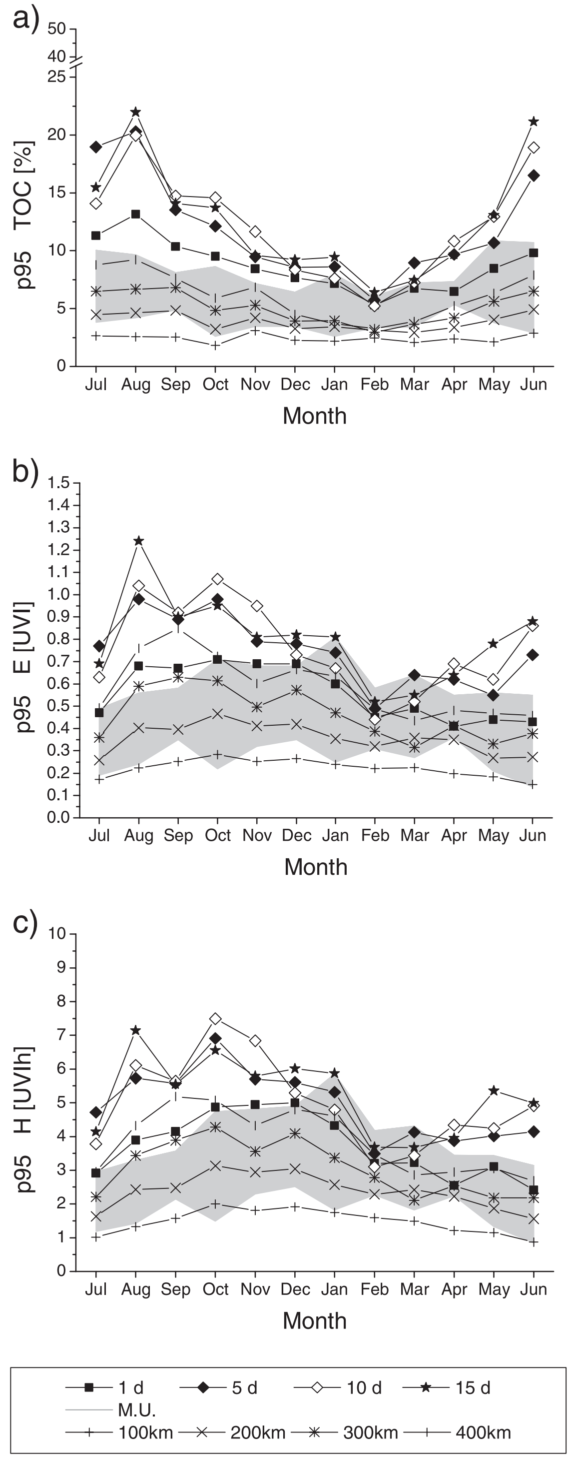

Figure 11. Ninety-fifth percentiles for absolute differences in total ozone p95ΔTOC (a), for irradiance at solar noon p95ΔE (b) and for daily dose p95ΔH (c) at 30.0°S, 18.1°E for certain temporal lags up to 15 days. The gray area indicates the measuring uncertainties of TOC and their influence on the erythemally effective UV radiation after Schmalwieser *et al.* (3). Shown are also the p95 values caused by the spatial (latitudinal) variability in TOC after Schmalwieser *et al.* (4).

obvious during the first months of the year. The p95 values in TOC caused by time lags are two times higher than those in summer. The annual course of measurement uncertainties remains relatively smooth. The difference in the annual courses is similar at 30°S. At the equator one can rather suspect the difference in the annual patterns.

In another preceding paper (4) we examined the influence of spatial variability in TOC values. At 50°N the p95 values due

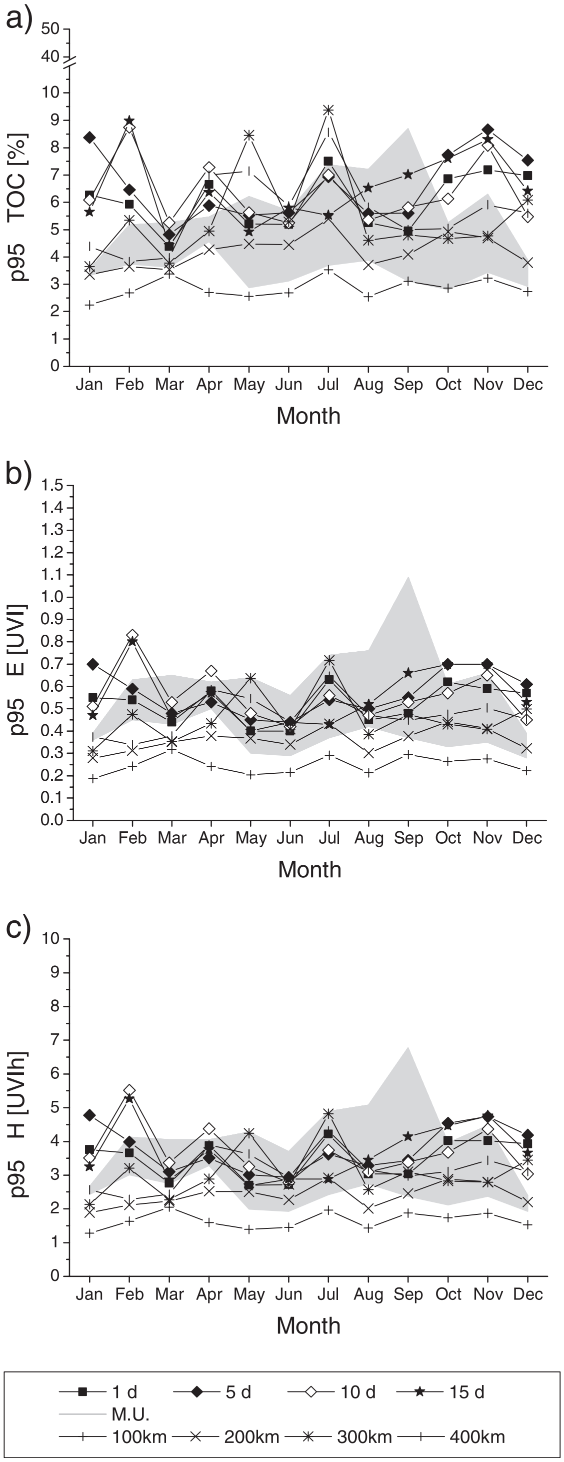

Figure 12. Ninety-fifth percentiles for absolute differences in total ozone p95ΔTOC (a), for irradiance at solar noon p95Δ*E* (b) and for daily dose p95Δ*H* (c) at 0.0°S, 36.6° for certain temporal lags up to 15 days. The gray area indicates the measuring uncertainties of TOC and their influence on the erythemally effective UV radiation after Schmalwieser *et al.* (3). Shown are also the p95 values caused by the spatial (latitudinal) variability in TOC after Schmalwieser *et al.* (4).

to a delay in TOC availability of 1 day is comparable with p95 values that are caused by spatial distances (latitude) between 400 and 500 km (Fig. 10). At 30°S a time lag of 1 day is comparable with spatial gaps of 300–400 km (Fig. 11). At the equator a delay of 1 day causes comparable p95 values as a gap of 200–300 km (Fig. 12).

From these sensitivity studies on spatial, temporal and measurement uncertainties it becomes evident that the most critical parameter for the accuracy of calculated UVI and daily dose values is the temporal resolution. Measurement uncertainties have a remarkable influence on the accuracy, too. The influence of a spatial resolution of 100 km (approximately 1° × 1°) is clearly smaller than that of the two others.

In order to minimize uncertainties by temporal total ozone variability for proposed and published UV values for the next day, forecasting of total ozone is crucial. Total ozone forecasts can be derived on a global basis by assimilating total ozone observations from satellites (*e.g.* EPTOMS or the Global Ozone Monitoring Experiment 2 aboard MetOp) into global chemistry transport models (42,43). The daily resulting total ozone analysis can then be used as the initial condition for the forecasting procedure driven by temperature- and windfields (*e.g.* from the European Center for Medium Range Weather Forecast).

REFERENCES

1. Weihs, P. and A. R. Webb (1996) Comparison of Green and Lowtran radiation schemes with a discrete ordinate method UV model. *Photochem. Photobiol.* **64**, 642–648.
2. Schwander, H., P. Koepke and A. Ruggaber (1997) Uncertainties in modeled UV irradiances due to the limited accuracy and availability of input data. *J. Geophys. Res.* **102**, 9419–9429.
3. Schmalwieser, A. W., G. Schauberger, T. Erbertseder, M. Janouch, G. J. R. Coetzee and P. Weihs (2007a) Sensitivity of erythemally effective UV irradiance and daily exposure to uncertainties in measured total ozone. *Photochem. Photobiol.* **83**, 434–444.
4. Schmalwieser, A. W., T. Erbertseder, G. Schauberger and P. Weihs (2008) Sensitivity of erythemally effective UV irradiance and daily exposure to spatial gaps in total ozone measurements. *Photochem. Photobiol.* (in press).
5. Dobson, G. M. B. and D. N. Harrison (1926) Measurements of the amount of ozone in the earth's atmosphere and its relation to other geophysical conditions. *Proc. R. Soc. Meteorol. Lond. A* **110**, 660–693.
6. Dobson, G. M. B., A. W. Brewer and B. M. Cwilong (1946) Meteorology of the lower stratosphere. *Proc. R. Meteorol. Soc. Lond.* **185**, 144–175.
7. Meetham, A. R. (1937) The correlation of the amount of ozone with other characteristics of the atmosphere. *Quart. J. R. Meteorol. Soc.* **63**, 289–307.
8. Reed, R. J. (1950) The role of vertical motions in ozone-weather relationship. *J. Atmos. Sci.* **7**, 263–267.
9. Schmalwieser, A. W., G. Schauberger, P. Weihs, R. Stubi, M. Janouch, G. J. R. Coetzee and S. Simic (2003) Preprocessing of total ozone content as an input parameter to UV Index forecast calculations. *J. Geophys. Res.* **108**, 4176–4189.
10. Haigh, J. (1996) The impact of solar variability on climate. *Science* **272**, 981–984.
11. Zerefos, C. S., K. Tourpali, B. R. Bojkov, D. S. Balis, B. Rognerud and I. S. A. Isaksen (1997) Solar activity-total column ozone relationships: Observations and model studies with heterogeneous chemistry. *J. Geophys. Res.* **102**, 1561–1569.
12. Labitzke, K., J. Austin, N. Butchart, J. Knight, M. Takahashi, M. Nakamoto, T. Nagashima, J. Haigh and V. Williams (2002) The global signal of the 11-year solar cycle in the stratosphere: Observations and models. *J. Atmos. Solar Terr. Phys.* **64**, 203–210.
13. Zerefos, C. S., A. Bais, I. C. Ziomas and B. R. Bojkov (1992) On the relative importance of Quasi-Biennial Oscillation and El Nino Southern Oscillation in the revised Dobson Total Ozone records. *J. Geophys. Res.* **100**, 10135–10144.

14. Funk, J. P. and G. L. Garnham (1962) Australian ozone observations and a suggested 24-month cycle. *Tellus* **14**, 378–382.
15. Bojkov, R. D. and V. E. Fioletov (1995) Estimating the global ozone characteristics during the last 30 years. *J. Geophys. Res.* **100**, 16537–16551.
16. Kane, R. P., Y. Sahai and N. R. Teixeira (1998) Latitude dependence of the quasi-biennial oscillation and quasi-triennial oscillation characteristics of total ozone measured by TOMS. *J. Geophys. Res.* **103**, 8477–8490.
17. Hasebe, F. (1980) A global analysis of the fluctuation of total ozone. II. Non-stationary annual oscillation, quasi-biennial oscillation and long-term variations in total ozone. *J. Meteorol. Soc. Jpn* **58**, 104–110.
18. Angell, J. K. (1997) Estimated impacts of Agung, El Chichon, and Pinatubo volcanic eruptions on global and regional total ozone after adjustment for the QBO. *Geophys. Res. Lett.* **24**, 647–650.
19. Nikulin, G. N. and R. P. Repinskaya (2001) Modulation of total ozone anomalies in the midlatitude Northern Hemisphere by the arctic oscillation. *Atm. Oceanic Phys.* **37**, 633–643.
20. Schnadt, C. and M. Dameris (2003) Relationship between North Atlantic Oscillation changes and stratospheric ozone recovery in the Northern Hemisphere in a chemistry-climate model. *Geophys. Res. Lett.* **30**(9), 1487, doi: 10.1029/2003GL017006.
21. Appenzeller, C., A. K. Weiss and J. Staehelin (2000) North Atlantic Oscillation modulates total ozone winter trends. *Geophys. Res. Lett.* **27**, 1134–1138.
22. Orsolini, Y. J. and V. Limpasuvan (2001) The North Atlantic Oscillation and the occurrence of ozone miniholes. *Geophys. Res. Lett.* **28**, 4099–4102.
23. International Commission on Non-Ionizing Radiation Protection (1995) *Global Solar UV Index—WHO/WMO/INCIRP Recommendation*. INCIRP publication No. 1/95. ICNIRP, Oberschleissheim, Germany.
24. World Health Organization (2002) *Global Solar UV Index: A Practical User Guide*. WHO, Geneva, Switzerland.
25. Commission Internationale de l'Eclairage (2003) *International Standard Global Solar UV Index*. CIE Standard S 013:2003. CIE, Vienna, Austria.
26. Vanicek, K., Z. Lytinska, T. Frei and A. Schmalwieser (2000) *UV Index for the Public*. Publication of the European Communities, Brussels, Belgium.
27. European Commission (2006) *Measurements and Assessment of Personal Exposure to Incoherent Optical Radiation—Part 3: UV-Radiation Emitted by the Sun*. European Pre-Standard prEN 14255-3:2006. European Commission, Brussels, Belgium.
28. Saxebøl, G. (2000) UVH—A proposal for a practical unit for biological effective dose for ultraviolet radiation exposure. *Radiat. Prot. Dosimetry* **88**, 261.
29. McPeters, R. D., P. K. Bhartia, A. J. Krueger, J. R. Herman, C. G. Wellemeyer, C. J. Seftor, G. Jaross, O. Torres, L. Moy, G. Labow, W. Byerly, S. L. Taylor, T. Swissler and R. P. Cebula (1998) *Earth Probe Total Ozone Mapping Spectrometer (TOMS) Data Products User's Guide*. NASA Reference Publication. NASA, Greenbelt, MD.
30. Wellemeyer, C. G., P. K. Bhartia, S. L. Taylor, W. Qin and C. Ahn (2004) Version 8 Total Ozone Mapping Spectrometer (TOMS) Algorithm. Available at: http://macuv.gsfc.nasa.gov/doc/toms_algor.pdf. Accessed on 4 August 2008.
31. Schauberger, G., A. W. Schmalwieser, F. Rubel, Y. Wang and G. Keck (1997) UV-index: operationelle Prognose der solaren, biologisch-effektiven Ultraviolett-Strahlung in Österreich. *Z. Med. Phys.* **7**, 153–160.
32. Diffey, B. L. (1977) The calculation of the spectral distribution of natural ultraviolet radiation under clear day conditions. *Phys. Med. Biol.* **22**, 309–316.
33. Bener, P. (1972) *Approximate Values of Intensity of Natural Radiation for Different Amounts of Atmospheric Ozone*. Eur. Res. Off., US Army, London, UK.
34. Schmalwieser, A. W., G. Schauberger, M. Januch, M. Nunez, T. Koskela, D. Berger, G. Karamanian, P. Prosek and K. Laska (2002) Global validation of a forecast model for irradiance of the solar, erythemally effective UV radiation. *Opt. Eng.* **40**, 3040–3050.
35. Commission Internationale de l'Eclairage (1987) A reference action spectrum for ultraviolet induced erythema in human skin. *CIE J.* **6**, 17–22.
36. Commission Internationale de l'Eclairage (1998) *Erythema Reference Action Spectrum and Standard Erythema Dose*. CIE S007E-1998. CIE, Vienna, Austria.
37. Koepke, P., A. Bais, D. Balis, M. Buchwitz, H. de Backer, X. de Cabo, P. Eckert, P. Eriksen, D. Gillotay, T. Koskela, B. Lapeta, Z. Litynska, J. Lorente, B. Mayer, A. Renaud, A. Ruggaber, G. Schauberger, G. Seckmeyer, P. Seifert, A. Schmalwieser, H. Schwander, K. Vanicek and M. Weber (1998) Comparison of models used for UV index calculations. *Photochem. Photobiol.* **67**, 657–662.
38. Schmalwieser, A. W. and G. Schauberger (2000) Validation of the Austrian forecast model for solar, biologically-effective ultraviolet radiation-UV index for Vienna. *Austria. J. Geophys. Res.* **105**, 26661–26668.
39. De Backer, H., P. Koepke, A. Bais, X. de Cabo, T. Frei, D. Gillotay, Ch. Haite, A. Heikkilä, A. Kazantzidis, T. Koskela, E. Kyrö, B. Lapeta, J. Lorente, K. Masson, B. Mayer, H. Plets, A. Redondas, A. Renaud, G. Schauberger, A. Schmalwieser, H. Schwander and K. Vanicek (2001) Comparison of measured and modelled UV indices for the assessment of health risks. *Meteor. Appl.* **8**, 267–277.
40. Schmalwieser, A. W., G. Schauberger, M. Janouch, M. Nunez, T. Koskela, D. Berger and G. Karamanian (2005) Global forecast model to predict the daily dose of the solar erythemally effective UV radiation. *Photochem. Photobiol.* **81**, 154–162.
41. Fitzpatrick, T. B., M. A. Pathak, L. C. Harber, M. Seiji and A. Kukita (1974) *Sunlight and Man*. University of Tokyo Press, Tokyo, Japan.
42. Eskes, H., P. van Velthoven, P. Valks and H. Kelder (2003) Assimilation of GOME total ozone satellite observations in a three-dimensional tracer transport model. *Q. J. R. Met. Soc.* **129**, 1663.
43. Baier, F., T. Erbertseder, O. Morgenstern, M. Bittner and G. Brasseur (2005) Assimilation of MIPAS observations using a three-dimensional chemical-transport model. *Q. J. R. Met. Soc*, **131**, 3529–3542.